

Comparison of Conduction Based and Mediator Based Models for Microbial Fuel Cells

R. Sedaqatvand, M. Nasr Esfahany*, T. Behzad & M.M. Mardanpour

Department of Chemical Engineering, Isfahan University of Technology, Isfahan, 8415683111, Iran
Mnasr@cc.iut.ac.ir

Abstract

Microbial fuel cells (MFCs) are processes used for simultaneous bioenergy capturing and waste treatment. In this study, a model for MFCs based upon a conduction mechanism for electron transfer is proposed, which integrates substrate utilization, current production and conduction and microbial distribution and growth in batch flow mode. The outputs of the model and that of a mediator based model are compared with respect to reference experimental results under a well controlled conditions using time evolution of produced current. The comparison shows that the electron shuttling mechanism appears to fail to predict the experimental data accurately enough while the conduction based model is able to reproduce measurements consistently.

Key words: Microbial Fuel Cell, Modeling, Conduction Based, Mediator Based, Batch Flow Mode.

Introduction

In recent years, with the depletion of the fossil fuel resources and emergence of environmental concerns, attempts have been made to look for so called green energies. Microbial fuel cells (MFCs) directly convert the bond energy in organics and inorganics to electrical energy. The fundamental performance resembles the conventional fuel cells, but their fuels are undesirable organics like wastewaters. Microorganisms play the role of biocatalysts in MFCs. They consume organics and subsequently produce electricity while eliminating contaminants. MFCs have advantage over the anaerobic digestion biogas technology. They are capable of using low strength wastewaters, which are not suitable for biogas processes [1]. Recent studies show increased values for current and power densities, which can lead to promising future for simultaneous wastewater treatment and power production [1-3]. In general, two major mechanisms are recognized up to now for electron transfer from cells to anode surface.

1. using externally added or endogenous mediators by which electrons transfer by means of redox reactions and diffusion.
2. Forming an electrical conductive medium by microbial community in which the electrons are transferred to

the anode by nanowires or direct contact under an electrical potential gradient [4; 5].

Furthermore, bacterial cells could be present in suspended form or attached biofilm to the anode surface. Although experimental data are valuable in determining mechanisms involved in a physical phenomenon, it is impossible to determine the design parameters quantitatively, without a mathematical model. Modeling studies in MFCs are very limited. The modeling studies could be divided into two major categories according to e⁻ transfer mechanisms. Marcus et al. (2007) [6] presented a conduction based model using biofilm formed on anode of a MFC to predict the performance. Picioreanu et al. (2007) [7] considered the mediator based electron transfer mechanism and presence of suspended biomass besides attached biofilm in their model. The role of flow hydrodynamics and pH were also investigated by the same research group in 2010 [8]. Although it is a notion now that the main electron transfer mechanism in most biofilms does not rely on externally added mediators [9; 10], Picioreanu et al. persisted on the same assumption of electron transfer in their recent modeling [11]. Furthermore, it was shown that biofilms have the main role in current production compared to the suspended cells [10].

In this study, conduction based e- transfer and only attached biofilms are considered to model the performance of a MFC. In this modeling, the anode compartment is considered and the effects of cathodic compartment and electrolyte are ignored. Hence, the anode electrical potential is poised at a fixed value by a potentiostat.

Several limitations influence the current production in MFCs, including substrate concentration gradient, electrical potential gradient [6], and pH variation through biofilms [12]. In this work, the first two limitations have been considered by employing a dual limitation rate equation for substrate utilization and current production. The produced current in anode is used as an important indication for MFC performance.

Since the conductive biofilm attaches to anode surface, it could be considered as an extension of anode surface and is called the “biofilm anode” [6]. The biofilm anode, here, consists of exoelectrogen microbes, which could transfer the produced electron in their respiratory chain out of their cells [2]. A subset of exoelectrogens, which are capable of using anode as their final electron acceptor and conduct electrons directly to the anode surface are referred to as “anode respiring bacteria (ARB)” [6; 13].

The main goal of this study is to compare conduction based and mediator based models for microbial fuel cells. This comparison is accomplished by using the experimental results presented in [9] as the reference data. The output of the models are compared and analyzed with respect to these results. The acetate and microbial species of *Geobacter Sulfurreducens* were used as substrate and the pure culture in biofilm, respectively. The experiments were conducted in batch flow mode and at poised anode potential of 0.2 (V) relative to Ag/AgCl standard electrode. The time evolution of produced current has been presented in a time period of eight days [9]. This is illustrated in figure 1 by black circles. There are two sudden rises in current level at dayes 4 and 5. This is due to the fresh substrate addition after its depletion, 1mM acetate each. Picioreanu et al. (2007) [7] presented a comprehensive model for microbial fuel cells based on the added mediators for electron transfer using similar conditions as in [9]. The model’s output is represented by dashed line in figure 1. At first, the acetate concentration was 1mM and the same concentration was injected on the fourth and fifth days to stimulate the biofilm anode. The current starts to decrease more quickly than experimental current in the third peak. The reason for this discrepancy in figure 1 will be explored in the next sections.

Model Structure

In this study, a dual limitation rate equation is considered for substrate utilization. In this case, electron donor (ED) and electron acceptor (EA) concentration control the rate of process under specific conditions. In contrast with mediator based formulation, EA is the solid conductive matrix of biofilm. For a non-soluble EA, the electrical potential represents the limiting effect of electron accep-

tor in biofilm anode instead of concentration. These concepts are described by Nernst-Monod term in rate equation. Equation 1 represents the dual limitation substrate utilization rate in dimensionless form adopted from [6].

$$q^* = \phi_a \left(\frac{S_d^*}{S_d^* + 1} \right) \left(\frac{1}{1 + \exp\left(-\frac{F V_{anod}}{RT} \eta^*\right)} \right) \quad (1)$$

where $q^* = q/q_{max}$, $S_d^* = S_d/K_{sd}$ and $\eta^* = \eta/V_{anod}$ is dimensionless form of $\eta = E_{anod} - E_{KA}$. E_{KA} is the potential at which one half of maximum rate is established.

Endogenous respiration process is responsible for electron generation from self oxidation of biomass [14]. Thus, the rate expression may be described as equation 2 in a similar way:

$$r_{res}^* = \phi_a \left(\frac{1}{1 + \exp\left(-\frac{F V_{anod}}{RT} \eta^*\right)} \right) \quad (2)$$

where $r_{res}^* = r_{res}/b_{res}$

Active biomass becomes inactive as expressed in equation (3):

$$r_{ina}^* = \phi_a \quad (3)$$

where $r_{ina}^* = r_{ina}/b_{ina}$

Biofilm anode is regarded as a linear conductor and is described by Ohm’s law [15]:

$$j = \frac{\kappa_{bio} V_{anod} \partial \eta^*}{L_f \partial \zeta} \quad (4)$$

Substrate utilization and endogenous respiration contribute to electron generation [14]. The steady state electron balance is represented by the following equation in dimensionless form [6]:

$$\frac{\kappa_{bio} V_{anod} \partial^2 \eta^*}{L_f^2 \partial \zeta^2} - \frac{F \gamma_1}{\tau} f_s^0 X_{f,a} q_{max} q^* - \frac{F \gamma_2}{\tau} X_{f,a} b_{res} r_{res}^* = 0 \quad (5)$$

The first term describes electron conduction and the second and third terms are electron source terms due to a substrate consumption and endogenous respiration, respectively.

The potential at anode surface is equal to anode potential poised by potentiostat and the current could not be conducted at biofilm/liquid interface. Thus, the boundary conditions are as follows [6]:

$$\eta^* |_{\zeta=0} = 1 \quad (6)$$

$$\frac{\partial \eta^*}{\partial \zeta} |_{\zeta=1} = 0 \quad (7)$$

Substrate is consumed by microorganisms as it diffuses through the biofilm. The dimensionless diffusion utilization equation for substrate is also in the form of equation (8):

$$\frac{D_{ED,f} K_{sd} \partial^2 S_d^*}{L_f^2 \partial \zeta^2} - X_{f,a} q_{max} q^* = 0 \quad (8)$$

The anode surface is impermeable with respect to substrate indicating zero flux boundary condition (eq. (9)). Also, no reaction occurs in diffusion layer adjacent to the biofilm. The substrate molar flux through the diffusion layer thus remains constant and is equal to the flux established at the biofilm interface. Using film theory, this boundary condition is described by eq. (10):

$$\frac{\partial S_d^*}{\partial \zeta} \Big|_{\zeta=0} = 0 \quad (9)$$

$$\frac{D_{ED,l}}{L} (S_{d,bulk}^* - S_{d,interface}^*) = D_{ED,f} \frac{\partial S_d^*}{\partial \zeta} \Big|_{\zeta=1} \quad (10)$$

where $S_{d,interface}^*$ is dimensionless substrate concentration at biofilm/liquid interface.

Equations 5 and 8 are considered steady state, because the time scale of diffusion, chemical reactions and electron conduction are small enough compared to those in biological processes. Thus, they can be imagined to occur in frozen state of biofilm distribution and growth [6].

Biofilms governed by Nernst-Monod equation possess a high electrical conductivity [13]. This improves the convergence rate significantly because the potential over the biofilm could be equated with that of anode with a negligible error. Thus, the Nernst-Monod term is fixed and nonlinear equations of 5 and 8 would be uncoupled. By assuming perfect mixing in anodic chamber, the temporal variation of bulk substrate concentration could be expressed by equation (11) in the batch mode:

$$\frac{V_a K_{Sd} v_{Lf}}{L_f} \left(\frac{dS_{d,bulk}^*}{dt^*} \right) = -A_s J_s \quad (11)$$

where J_s is the molar flux of substrate entering into the biofilm. This term indicates the substrate consumption by bioelectrochemical reaction inside the biofilm.

Two types of bacterial species are considered here which compete for space [16]. Active biomass, which functions as biocatalyst and electron generator and inactive biomass, which mainly accounts for the conductive matrix. A fraction of generated electrons (Y) is utilized for new active biomass synthesis. On the other hand, it is decayed by endogenous respiration and inactivation mechanisms [14]. The inactivation is also the main generator of inert biomass. The transient one dimensional and multi species mass balance for active and inactive biomass could be adopted from Wanner and Gujer (1986) [17]:

$$\frac{\partial \phi_a}{\partial t^*} + \frac{\partial (v^* \phi_a)}{\partial \zeta} = \frac{Y q_{max} L_f}{v_{Lf}} q^* - \frac{b_{res} L_f}{v_{Lf}} r_{res}^* - \frac{b_{ina} L_f}{v_{Lf}} r_{ina}^* \equiv \mu_a \quad (12)$$

$$\frac{\partial \phi_i}{\partial t^*} + \frac{\partial (v^* \phi_i)}{\partial \zeta} = \frac{X_{f,a} b_{ina} L_f}{X_{f,i} v_{Lf}} r_{ina}^* \equiv \mu_i \quad (13)$$

$$\Phi + \Phi \alpha \quad (14)$$

where $v^* = v / v_{Lf}$

The left hand sides of equations 12 and 13 describe the accumulation and convection of biomass as a result of net generation of active and inactive biomass, respectively. The microbes could not move into anode electrode, therefore the zero convective flux boundary conditions for both equations 12 and 13 may be expressed as:

$$v^* \Big|_{\zeta=0} = 0 \quad (15)$$

All above contributions result in a net growth rate for biofilm and its movement in perpendicular direction to immobile anode surface with the advective velocity of v , which is described by equation [16]. Regarding this impact, the bacterial transfer in biofilm is dominated by convection only.

$$v^*(t, \zeta) = \frac{1}{v_{Lf}} \int_0^1 (\mu_a + \mu_i) L_f d\zeta \quad (16)$$

The biofilm thickness changes with time in response to the net growth rate and detachment as described in equation [17]. Detachment is caused by shear stress associated with flowing bulk liquid and sloughing off the biofilm.

$$\frac{dL_f}{dt} = v(t, L_f) - b_{det} L_f \quad (17)$$

All above differential equations are spatially discretized by finite difference method [18]. The nonlinear equations are solved by trust region method based on interior reflective Newton [19]. Also, the unsteady state equations are discretized temporally by method of line and implicit Euler [18]. After determining concentration and potential profiles by solving equations 8 and 5, respectively, advective velocity at biofilm interface could be calculated from eq. 16. The bulk concentration in eq. 10 is replaced by updated value, which is determined by solving eq. 11. Then, the bacterial distribution over biofilm and biofilm thickness are computed by solving equations 12, 14 and 17, respectively. This procedure continues repeatedly until the current calculated from eq 4 sustains. The model is implemented by MATLAB software. Acetate is used as electron donor and the biofilm is composed of G.Sulfurreducens, an anode respiring bacteria.

Results and Discussion

As mentioned earlier, there was a relatively high deviation between simulation results of the mediator based model [7] and experimental data [9] as shown in figure 1. The calculated current from mediator based model falls to basal level more rapidly than experimental measurements. This could be explained by electron shuttle diffusion limitation in thicker biofilm as considered in the mediator based models [7; 11].

Using the parameters listed in table 1, conduction based model described in this work was solved. The parameters are mainly adopted from the literature and some of them, which belong to the present model, are varied in their specific range.

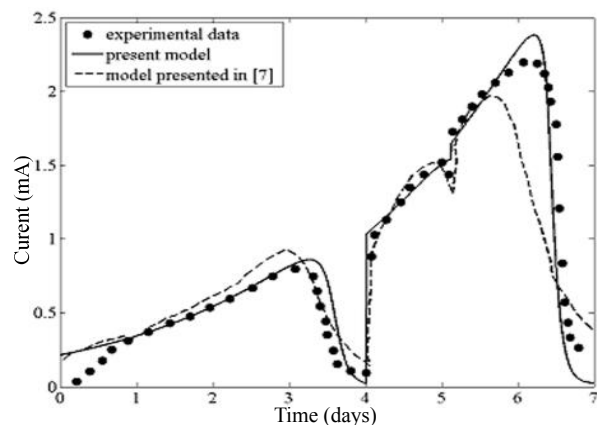


Figure 1. Time evolution of produced current based on experimental data [9] (circles), conduction based model (solid line) and the model presented in [7] (dashed line) for initial acetate concentration of 1mM and two stimuli at days 4 and 5 with the same coccentration

Table 1. Model parameters values used to reproduce the experimental data from [9]

symbol	unit	value	reference	symbol	unit	value	reference
K_{sd}	mmol cm ⁻³	1.563*10 ⁻⁵	[7]	X_{fa}, X_{fi}	mgVS cm ⁻³	211.9	[7]
q_{max}	mmol mgVS ⁻¹ day ⁻¹	0.2	[7]	Y	mgVS mmolED ⁻¹	3.074	[14]
L	cm	0.02	assumed	f_e^0	dimensionless	0.95	[14]
b_{res}	day ⁻¹	0.07	assumed	$S_{d,bulk}^0$	mM	1	[9]
b_{ina}	day ⁻¹	0.02	assumed	E_{KA}	V	-0.448	[13]
b_{det}	day ⁻¹	0.05	assumed	A_s	cm ²	61.2	[9]
$D_{ED,l}$	cm ² day ⁻¹	0.941	[6]	γ_1	mmole ⁻¹ mmolED ⁻¹	8	[14]
$D_{ED,f}$	cm ² day ⁻¹	0.753	[14]	γ_2	mmole ⁻¹ mgVS ⁻¹	0.177	[14]
κ_{bio}	mS cm ⁻¹	0.5	[13]	V_{anod}	V	0.2	[9]

The output of the model is represented in figure 1 using the parameter values in table 1. Furthermore, the corresponding experimental values and mediator based model predictions are also shown in the figure.

The current starts to increase from its initial value as the biofilm grows on the anode surface and the substrate is oxidized. By electricity production in anode, the substrate concentration reduces continuously and falls to zero in batch flow mode. Subsequently, the produced current is also reduced and reaches to a basal level until the fresh substrate would be added and current rises again. If a developed and mature biofilm exists over the anode surface, the current will repeat its behavior in successive substrate injections and gain the same maximum level; otherwise it will be higher than the previous current level.

In figure 1, fresh substrate is supplied for the biofilm on the fourth and fifth days. The current levels rise immediately in these times and are different from the last current level before stimuli. The current level growth is exponential as the biofilm is developing from its initial state [9]. The model described here is superior to model offered by Picioareanu et al. (2007) [7] in predicting the current evolution.

It is to be noted that mediator based model failed to predict current evolution after fifth day whereas the present model predictions show excellent agreement with the experimental measurements during the whole period under investigation. The maximum attainable current predicted in [7] is about 10% lower than the measured one. The predicted current by mediator based model deviates approximately 42% from the measured current on the sixth day, when the experimental current reaches its maximum.

The deviation in the results of mediator based model and experiments could be due to the assumption of electron transfer by mediators and its associated limitations imposed to the current production. This effect causes the mediator based model to predict higher current in initial phases before day 4 [7]; while the present model is able to predict the measured current nicely.

Figures 2-(a and b) show the evolution of the bulk substrate concentration and biofilm thickness, respectively. The biofilm thickness declines from its initial value (2.5 μm) because of the existence of decay mechanisms and the substrate diffusion limitations, which hinder the efficient nutrient delivery to the mi-

crobs. After the second day, biofilm starts to grow until the substrate depletion causes it to reduce again. By the first substrate injection on the fourth day and nutrient provided, the biofilm grows rapidly and becomes 2.83 μm thick. Again, biofilm thickness reduces by approximately 4 μm due to complete substrate depletion. This quick rise in biofilm thickness may account for greater produced current in the last peak in figure 1.

The substrate concentration variation in time is also represented in figure 2a. Substrate is gradually consumed by the biofilm and its concentration falls to zero on the fourth day. The first substrate injection occurs at the fourth day and causes the substrate concentration to increase abruptly. In the second substrate injection on the fifth day, the substrate is not completely depleted and 1 mM acetate is added to the anodic chamber. In both injections, the concentration is reduced linearly as current produced.

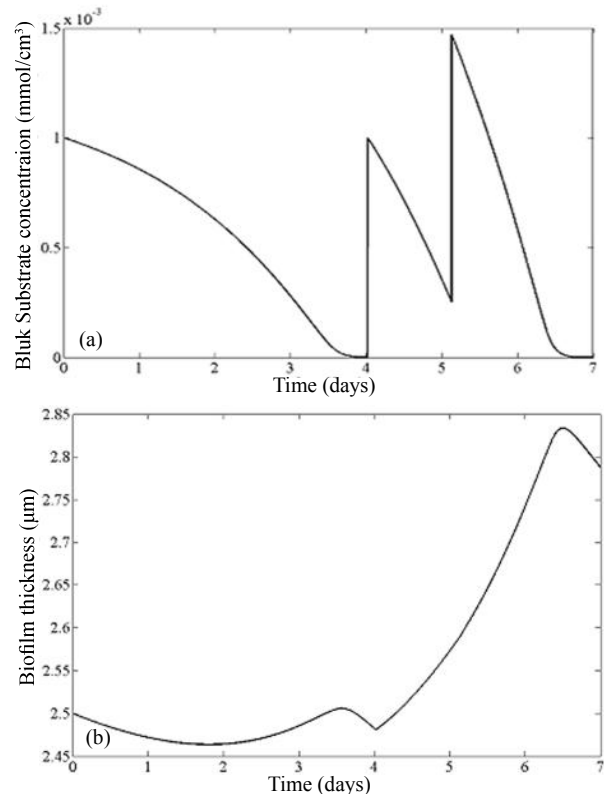


Figure 2. a) Variation of substrate concentration and b) biofilm thickness in time for initial acetate concentration of 1 mM and two stimuli on days 4 and 5 with the same concentration for conduction based model

Figure 1 and figure 2a reveal that the current would be non-zero once the substrate concentration falls to zero on the fourth day. This is due to the biofilm self oxidation. In fact, active microbial species are oxidized by self oxidation phenomena and produce a basal current value in the absence of substrate. The value of basal current increases by endogenous respiration as shown in figure 3. The value of endogenous respiration rate constant rises to 0.14 day^{-1} with respect to what was considered in figure 1 and the related current time evolution is illustrated in figure 3. The basal current increases from 0.02 mA to 0.19 mA (8.5 fold increase) at fourth day as the respiration rate constant doubles. Doubling the respiration rate constant causes the active biomass to decay more rapidly and thus the maximum current levels reduce at each stimuli.

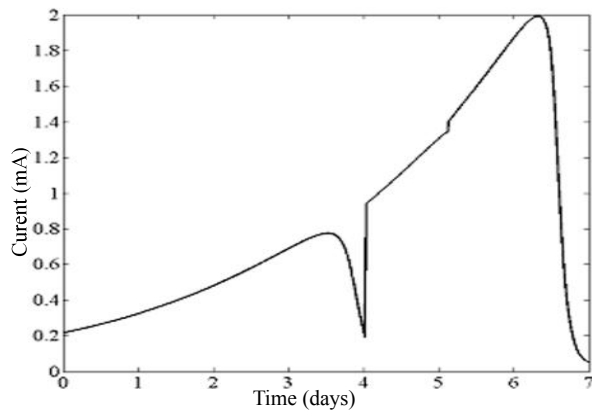


Figure 3. Effect of respiration constant increase to 0.14 day^{-1} in time evolution of the produced current based on conduction based model

The biomass distribution with respiration rate constant of 0.07 day^{-1} is also demonstrated in figure 4. The active and inert biomass distributions show negligible changes through biofilm thickness; thus, the vertical axis scales are modified by $((\square_0 - \square) / \square_0) * 10^3$ in order to magnify the microbes distribution (\square_0 is biomass volume fraction at $\zeta=0$). The active biomass accumulates mainly close to the biofilm surface and the inert biomass close to the anode surface. This could be due to the further access to nutrients for active biomass and further potentials for inert species.

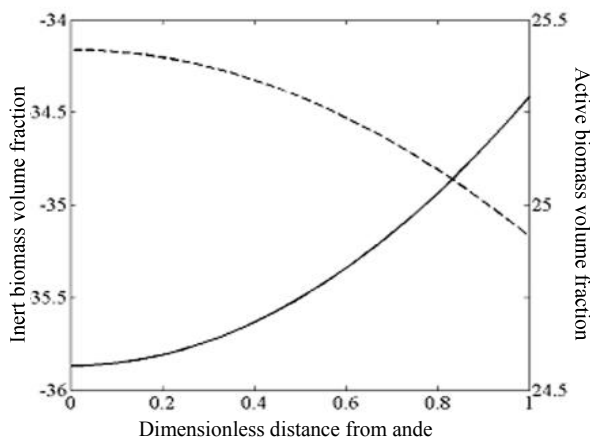


Figure 4. Biomass distribution through biofilm thickness on the seventh day

Conclusions

In this study, a MFC model based on conduction of the biofilm attached to the anode is adopted and modified such that the effects of substrate stimuli could be captured. Model's outputs along with the results of mediator based model are compared with respect to the experimental observations. This comparison revealed that the mechanism of electron shuttling seems to describe the process insufficiently and it is most likely that the electrons transfer by direct conduction in biofilms. The conduction based model is capable of predicting experimental measurements more accurately than the mediator based model. The predicted maximum attainable current by mediator based model is about 10% lower than the experimental measurement. Also, it deviated about 42% when the experimental current reaches its maximum. In contrast, the conduction based model calculates the maximum current in the last stimuli, at the same time as the current became maximum in experiments and demonstrates a deviation of approximately 7%. This deviation could be attributed to the uncertainties in parameter estimation. The basal current value increases by 8.5 times as the respiration rate constant doubles. The microbial species show a negligible distribution over biofilm thickness. The model described here is able to predict produced current, substrate removal flux, biofilm thickness and distribution, substrate concentration and electrical potential profiles, and dynamic behaviour of the system. Conduction based models for microbial fuel cells could establish a basis for further MFCs modeling studies and could be expanded for more microbial species and various substrates to describe more complicated and applicable MFCs.

Nomenclature

- b_{ina} : Inactivation rate constant (day^{-1})
- b_{det} : Detachment rate (day^{-1})
- b_{res} : Respiration rate constant (day^{-1})
- D_{ED} : ED diffusivity ($\text{cm}^2 \text{ day}^{-1}$)
- E_{anod} : Anodic potential (V)
- E_{KA} : Half saturation potential (V)
- F : Faraday's constant (96485 C/mol e^-)
- f_e^0 : fraction of e^- used for current
- j : Current density (mA cm^{-2})
- K_{sd} : Half saturation concentration (mmol cm^{-3})
- L : Diffusion layer thickness (cm)
- L_f : Biofilm thickness (cm)
- q : Specific ED consumption rate ($\text{mmol mgVS}^{-1} \text{ day}^{-1}$)
- q_{max} : Maximum Specific ED utilization rate ($\text{mmol mgVS}^{-1} \text{ day}^{-1}$)
- R : Gas constant ($\text{J mol}^{-1} \text{ K}^{-1}$)
- r_{res} : Endogenous respiration rate (day^{-1})
- r_{ina} : Inactivation rate (day^{-1})
- S_d : Substrate concentration (mmol cm^{-3})
- T : Temperature (K)
- J_s : Substrate molar flux ($\text{mmol cm}^{-2} \text{ day}^{-1}$)
- V_{anod} : Anode voltage (V)

X_f : Biofilm density (mgVS cm⁻³)
 Y : True yield (mgVS mmol⁻¹)
 k_{bio} : Bbiofilm conductivity (mS cm⁻¹)
 \square : Biomass volume fraction
 τ : Conversion factor (86400 s day⁻¹)
 γ_j : ED e⁻ equivalence (mol e⁻ mol ED⁻¹)
 γ_2 : Biomass e⁻ equivalence (mol e⁻ mgVS⁻¹)
 v_{L_f} : Velocity at biofilm interface (cm day⁻¹)
 ζ : Dimensionless distance (normalized by L_p)
 μ : Net specific biomass generation rate (day⁻¹)
 V_a : Anode chamber volume (cm³)
 A_s : Anode surface area (cm²)

Subscripts and superscripts

*: Dimensionless quantity

a : Active biomass

i : Inactive biomass

f : Biofilm

l : Liquid

bulk: Bulk liquid

References

- [1] Watanabe K., "Recent Developments in Microbial Fuel Cell Technologies for Sustainable Bioenergy", 2008, Journal of Bioscience and Bioengineering, Vol. 106, pp. 528–536.
- [2] Logan B.E., *microbial fuel cells*, Newyork : wiley, 2007.
- [3] Logan B.E. & Regan, J.M. "Microbial fuel cells: challenges and applications", Environmental Science & Technology, pp. 5172-5180. 2006.
- [4] Logan B.E, Hamelers B., Rozendal R., Schroder U., Keller, J., Freguia, S., Aelterman P., Verstraete W. & Rabaeay K., "Microbial Fuel Cells: Methodology and Technology", Environmental Science & Technology, Vol. 40, pp. 5181-5192, 2006.
- [5] Schroder U., "Microbial Fuel Cells", s.l. : Elsevier B.V., 2009.
- [6] Rittmann B.E., Conduction based Modeling of the Biofilm Anode of a Microbial Fuel Cell. Marcus, A.K., Torres, C.I., "Biotechnology and Bioengineering", Vol. 98, pp. 1171-1182, 2007.
- [7] Picioreanu C., Head I.M., Katuri K.P., van Loosdrecht M.C.M., Scott K., "A computational model for biofilm-based microbial fuel cells", Water Research, Vol. 41, pp. 2921-2940, 2007.
- [8] Picioreanu C., van Loosdrecht M.C.M., Curtis T.P. & Scott K., "Model based evaluation of the effect of pH and electrode geometry on microbial fuel cell performance", Bioelectrochemistry, pp. 8–24, 2010.
- [9] Lovley D.R. & Bond D.R., 2003, Applied and Environmental Microbiology, "Electricity Production by *Geobacter sulfurreducens* Attached to Electrodes", pp. 1548–1555.
- [10] Chaudhuri S.K. & Lovley D.R., "Electricity generation by direct oxidation of glucose in mediatorless microbial fuel cells", Nature Biotechnology, pp. 1-4, 2003.
- [11] Picioreanu C., Katuri K.P., van Loosdrecht M.C.M., Head I.M. & Scott K., "Modelling microbial fuel cells with suspended cells and added electron transfer mediator", Journal of Applied Electrochemistry, Vol. 40, pp. 151-162, 2010.
- [12] Torres C.I., Marcus A.K. & Rittmann, B.E., Proton Transport Inside the Biofilm Limits Electrical Current Generation by Anode-Respiring Bacteria, "Biotechnology and Bioengineering", Vol. 100, pp. 872-881, 2008.
- [13] Torres C.I., Marcus A.K., Parameswaran P. & Rittmann B.E., "Kinetic Experiments for Evaluating the Nernst-Monod Model for Anode-Respiring Bacteria (ARB) in a Biofilm Anode", Environmental Science & Technology, Vol. 42, pp. 6593-6597, 2008.
- [14] Rittmann B.E. & McCarty P.L., *Environmental Biotechnology, Principles and Applications*. s.l. : McGraw-Hill, 2001.
- [15] Bernardin D.M. & Verbrugge M.W. "Mathematical model of a gas-diffusion electrode bonded to a polymer electrolyte". 1991, AIChE journal, Vol. 37, pp. 1151-1163.
- [16] Rittmann B.E. & Manem J.A., "Development and experimental evaluation of a steady-state, multispecies biofilm model", Biotechnology and Bioengineering, Vol. 39, pp. 914–922, 1992.
- [17] Wanner O. & Gujer W., A multispecies biofilm model. , Biotechnology and Bioengineering, Vol. 28, pp. 314-328, 1986.
- [18] Constantinides A., Mostoufi N., *Numerical methods for chemical engineers with MATLAB application*, s.l. : Prentice Hall, 1999.
- [19] Coleman T.F. & Li Y., An Interior, "Trust Region Approach for Nonlinear Minimization Subject to Bounds", 1996, SIAM Journal on Optimization, Vol. 6, pp. 418-445.